

# Diff-Dagger: Uncertainty Estimation with Diffusion Policy for Robotic Manipulation

Sung-Wook Lee<sup>1</sup>, Yen-Ling Kuo<sup>1</sup>

**Abstract**—Recently, diffusion policy has shown impressive results in handling multi-modal tasks in robotic manipulation. However, it has fundamental limitations in out-of-distribution failures that persist due to compounding errors and its limited capability to extrapolate. One way to address these limitations is robot-gated DAgger, an interactive imitation learning with a robot query system to actively seek expert help during policy rollout. While robot-gated DAgger has high potential for learning at scale, existing methods like Ensemble-Dagger struggle with highly expressive policies: They often misinterpret policy disagreements as uncertainty at multi-modal decision points. To address this problem, we introduce Diff-Dagger, an efficient robot-gated DAgger algorithm that leverages the training objective of diffusion policy. We evaluate Diff-Dagger across different robot tasks including stacking, pushing, and plugging, and show that Diff-Dagger improves the task failure prediction by 37%, the task completion rate by 14%, and reduces the wall-clock time by up to 540%. We hope that this work opens up a path for efficiently incorporating expressive yet data-hungry policies into interactive robot learning settings. Project website: [diffdagger.github.io](https://diffdagger.github.io)

## I. INTRODUCTION

Imitation learning for manipulation tasks poses significant challenges due to the need for long-horizon decision making, high precision, and adaptability in dynamic environments. Recently, significant advances have been made using offline approaches, also known as behavior cloning, by adopting generative models for action sequence prediction. These models mitigate the compounding error issue by reducing the number of action inferences [1] and addressing multi-modality through generative capabilities [2]. In particular, diffusion policy [3] trains the model to predict the gradient of the action score function, and it has achieved state-of-the-art results for learning different robotic tasks.

While diffusion policy effectively handles highly multi-modal demonstrations, it still faces a core issue of behavior cloning: the out-of-distribution (OOD) failure, where the policy compounds errors in action prediction and cannot extrapolate in unseen states. A common strategy to address OOD failure is DAgger [4], an interactive learning method which iteratively refines the policy by incorporating expert interventions. In particular, robot-gated DAgger lets robots decide when to seek expert help, removing the need for constant human supervision and enabling large-scale learning across multiple robots [5]. The effectiveness of this approach, therefore, relies heavily on the robot’s ability to accurately estimate its own uncertainty.

However, none of the existing robot-gated DAgger approaches fully addresses the multi-modality present in

demonstration data. For example, the most widely adopted Ensemble-Dagger approaches use the action variance among an ensemble of policies to estimate uncertainty [6–8]. This means that when tasks admit multiple solutions, policies might erroneously indicate high uncertainty even when in a previously visited state. We illustrate this problem with a 2D navigation example (Figure 2 (a)), where two primary paths—clockwise and counterclockwise around a circle—lead to the goal. This scenario allows us to categorize regions as in-distribution uni-modal (along the circular paths, shown as mixed red and orange), in-distribution multi-modal (at the path divergence point, shown as green), and out-of-distribution (significant deviations from expected paths, shown as blue). While ensemble methods for robot-gated DAgger effectively distinguish in-distribution uni-modal from out-of-distribution data using action variance, they fail at in-distribution multi-modal points due to policy disagreement (Figure 2 (b)).

Incorporating an expressive policy class that handles multi-modal data into the DAgger framework is a promising but under-explored direction. In light of this, we propose Diff-Dagger, an efficient robot-gated DAgger algorithm that addresses multi-modality in demonstration data while reducing wall-clock time compared to other methods. Diff-Dagger uses a query system based on the loss function of the diffusion model, referred to as diffusion loss, which significantly improves the effectiveness of robot queries across various evaluation metrics. In three challenging manipulation tasks, Diff-Dagger achieves a 37% higher F1 score in predicting task failure, and the collected data leads to 14% improvements in policy performance while improving the wall clock time by 540% in comparison to the baseline methods.

We make the following contributions: First, we develop a novel robot-gated query system based on diffusion loss to handle multi-modality in expert demonstration. Second, we quantitatively evaluate Diff-Dagger’s efficiency in terms of task failure prediction, task completion, and wall-clock time during interactive learning to demonstrate its superiority over other baseline methods. Lastly, we discuss design choices that accelerate policy learning to enable faster convergence and improved overall performance.

## II. RELATED WORK

### A. Interactive Imitation Learning

The goal of imitation learning is to train a policy from an offline dataset through supervised learning. However, this approach suffers from a fundamental issue when the

<sup>1</sup>University of Virginia {dcs3zc, ylkuo}@virginia.edu

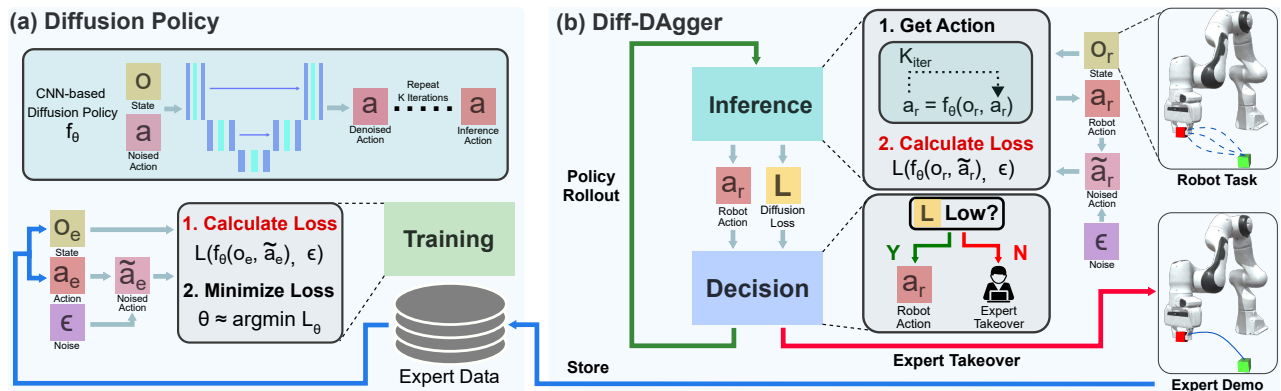


Fig. 1: **Overview of Diff-DaGger.** (a) **Diffusion Policy and Training:** In our study, we use the diffusion policy with a U-net architecture, a CNN-based model. During the training phase, diffusion policy is trained on static expert data. (b) **Diff-DaGger during Deployment:** At each timestep during the online learning phase, the robot performs two steps—**inference** and **decision**. In the inference step, the policy makes action inference by iteratively denoising a random noise, conditioned on the current observation. After action generation, the training loss function is used to compute the loss associated with the generated action. In the decision step, the robot proceeds with the action if the loss is low, otherwise it asks the expert to intervene. The arrows indicate the flow of steps.

policy distribution cannot perfectly match that of the expert distribution, also known as the covariate shift problem. [9]. Interactive imitation learning combats this issue through online expert intervention to recover from undesired states visited by the trained policy. One approach in interactive imitation learning is human-gated DAgger (HG-DAgger) [10], where a human supervisor decides when to correct a

robot’s actions. However, this requires continuous, one-on-one monitoring, making it resource-intensive and unscalable for parallel learning with multiple robots. The alternative method is called the robot-gated DAgger, which requires the robot to autonomously estimate its own uncertainty. A common challenge in interactive imitation learning is to maximize the utility of expert intervention while minimizing the burden on the expert.

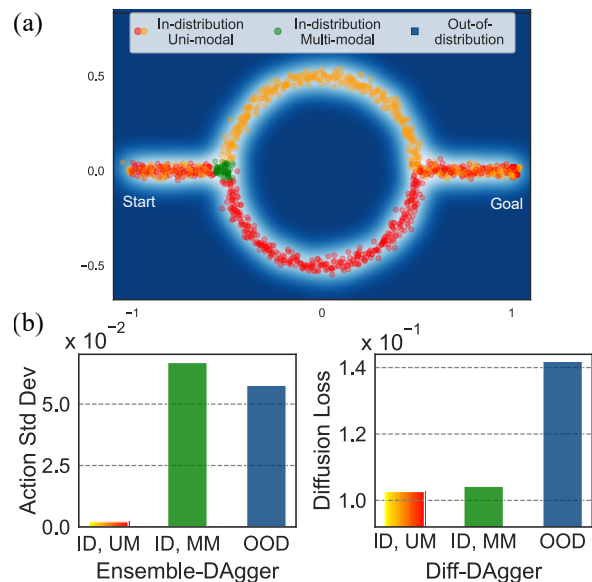


Fig. 2: (a) Visualization of 2D navigation toy example. The orange dots represent the mode for following a clockwise path around the circle and the red dots represent another mode for following a counter-clockwise path. The green dots represent the multi-modal region where multiple diverging paths exist. The blue region indicates out-of-distribution. (b) Comparison of action variance and diffusion loss for different regions across 100 runs in the 2D navigation example. The left bar plot displays the standard deviation of action across policies for in-distribution uni-modal (ID, UM), in-distribution multi-modal (ID, MM), and out-of-distribution (OOD) regions. The right bar plot shows the corresponding diffusion loss for these regions.

### B. Uncertainty Estimation of Robot Action

The most widely used method for estimating action uncertainty is to use an ensemble of policies bootstrapped on a subset of the training data and using the level of disagreement among the policies output to estimate uncertainty [6–8]. However, the ensemble method for uncertainty estimation can be problematic in practice, especially when the task allows multiple modes of completion. Specifically, they are prone to either mistaking in-distribution multi-modal data as out-of-distribution data or vice versa. This is because expressive ensemble policies may disagree due to the presence of multiple viable strategies where each policy is certain about its generated plan, leading to a high action variance. Furthermore, if the policy generates an action sequence instead of a single action, the uncertainty estimation may explode due to increasing divergence over time or lose accuracy if a shorter horizon is used for calculating action variance.

Another uncertainty estimation method is to use a separately trained classifier to more explicitly detect OOD states using failure states [11]. However, this requires significant efforts of collecting and labeling human-gated interventions as training data. In [12], the auxiliary reconstruction loss from the image observations is proposed to estimate uncertainty, but this method may be susceptible to confounding variables related to reconstruction complexity, potentially independent of the current state’s in-distribution status.

In contrast to the existing robot-gated DAgger methods, our approach addresses multi-modality in the demonstration

data by incorporating the loss function of diffusion policy into the decision rule. This approach does not need multiple policies for uncertainty estimation, reducing both training and inference time while benefiting from using an expressive policy class.

### C. Policy Learning and Classification with Diffusion Models

Diffusion models, originally proposed as generative models for images, have seen success in various decision-making tasks due to their ability to handle complex data distributions. In robotics, these models have been used in various aspects including reinforcement learning (RL) [13], imitation learning [3], task planning and motion planning [14]. Interestingly, diffusion models have also been shown to be effective zero-shot classifiers for the data distributions they are trained on [15–17]. This dual functionality of generative and discriminative capabilities enhances their value in decision-making tasks. Especially, it aligns well with a robot-gated DAgger framework, which requires both generation and evaluation of robot plans to decide when human intervention is necessary during task execution.

## III. METHOD

### A. Problem Statement

The goal of imitation learning is to collect a dataset and train a robot policy to complete a set of tasks with expert demonstrations. In the robot-gated DAgger scenario, the robot autonomously queries for expert intervention. We assume the expert is skilled in completing the task, which is considered successful if the goal is reached within the time limit. We assume access to success information. Our objective is to design an efficient robot query system that accurately predicts task failures, requesting expert intervention only when necessary.

### B. Diffusion Policy

1) *Action Diffusion*: In diffusion policy, robot behavior is generated through an iterative denoising process based on Langevin dynamics, formally modeled as a Denoising Diffusion Probabilistic Model (DDPM) [2]. This denoising process begins with a Gaussian prior,  $\mathcal{N}(0, I)$ , and iteratively removes noise to reconstruct the original data. Diffusion policy conditions on observation sequences and generates an action sequence, achieving state-of-the-art performance across various robotic tasks [3].

2) *Loss Function*: During training, diffusion policy samples a denoising timestep and a Gaussian noise vector to corrupt the action sequence. It then predicts the target objective given the corrupted action sequence and the observation sequence, and performs optimization by minimizing the following loss function:

$$L_\pi(o, a, \epsilon, t) = \|f(\epsilon, a) - f_\theta(o, \sqrt{\alpha_t}a + \sqrt{1 - \alpha_t}\epsilon, t)\|^2 \quad (1)$$

where  $o$  is the observation sequence,  $a$  is the action sequence, and  $\epsilon$  is a noise vector from Gaussian distribution  $\mathcal{N}(0, I)$ . The parameter  $\alpha_t$  is a time-dependent factor that modulates

the influence of the original data and the added noise during the diffusion process, and  $t$  is the denoising timestep. The loss function  $L(o, a, \epsilon, t)$  calculates the mean squared error (MSE) between the target variable  $f(\epsilon, a)$ , which is a function of noise and ground truth action depending on the choice of target prediction, and the noise predicted by the model  $f_\theta$ , given the noised data at time  $t$  [18].

### C. Diff-DAgger

1) *OOD Detection via Diffusion Loss*: During robot roll-out, the uncertainty of the current action plan is estimated using the diffusion policy’s loss value for the given observation and the generated action. In order to establish a baseline, we calculate the expected diffusion loss  $\mathcal{L}$  for each data point in the training dataset using equation 2.

$$\mathcal{L}(o, a, \pi) = \mathbb{E}_{\epsilon \sim \mathcal{N}(0, I), t \sim \mu(1, T)} L_\pi(o, a, \epsilon, t) \quad (2)$$

For practical implementation, we select a batch size  $N_b$  to sample both the noise and diffusion timesteps and compute the average loss over the batch. Given a quantile threshold  $\alpha$ , we assume OOD if the diffusion loss of the generated action using Eqn 2 exceeds the  $\alpha$ -quantile of the expected diffusion losses from the training data. Additionally, expert supervision takes place only if  $K$  past states consecutively violate the quantile threshold  $\alpha$ . It helps distinguish brief fluctuations from persistent out-of-distribution cases, significantly reducing the rate of false positives.

---

#### Algorithm 1 Diff-DAgger

---

```

1: Require Initial expert dataset  $D_{exp}$ , time-limit  $T_L$ , expert
   policy  $\pi_e$ , and thresholds  $\alpha$  and  $K$ 
2: Initialize diffusion policy  $\pi_r$  by training on  $D_{exp}$ 
3: for each trial do
4:   Train policy  $\pi_r$  on dataset  $D_{exp}$ 
5:   Set the threshold using  $D_{exp}$  and  $\alpha$ 
6:   control  $\leftarrow$  robot
7:   while task is not done do
8:     while control = expert and task is not done do
9:        $a_e \leftarrow \pi_e(o)$   $\triangleright$  Expert provides action
10:      Take action  $a_e$ 
11:       $D_{exp} \leftarrow D_{exp} \cup (o, a_e)$   $\triangleright$  Record state-action
12:    end while
13:     $a_r \leftarrow \pi_r(o)$   $\triangleright$  Policy provides action
14:    loss  $\leftarrow \mathcal{L}(o, a_r, \pi_r)$   $\triangleright$  Using Eq. 2
15:    if CDF(loss)  $<$   $\alpha$  for last  $K$  timesteps then
16:      control  $\leftarrow$  expert  $\triangleright$  Expert takeover
17:    else
18:      Take action  $a_r$ 
19:    end if
20:  end while
21: end for

```

---

2) *Data Aggregation and Policy Update*: We now summarize the data aggregation and policy update procedures. Diff-DAgger first initializes the policy  $\pi_r$  by training it on  $N_i$  initial expert demonstrations. After training the policy, the robot continues rolling out the action in the environment until high diffusion loss is detected. When the robot query is made, experts intervene from the current scene and complete the task. Upon completion of the task by either the robot or the

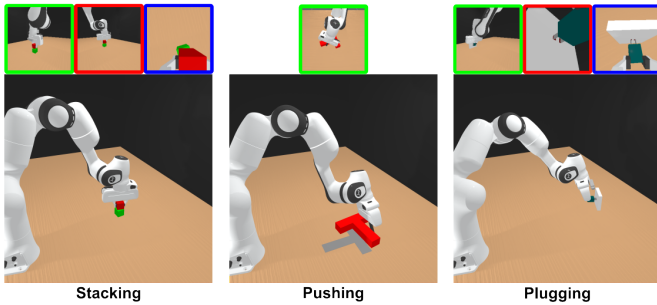


Fig. 3: Tasks (**Bottom**) and Camera Views (**Top**). For pushing, a single camera is used. For stacking and plugging, three cameras are used to account for occlusion and gripper motion.

Task	# Obj	Contact Rich	High-Fidel	$T_L$	Expert Type	Task Dur	Succ Rate
Stacking	2	False	False	250	Motion Planner	60.3	1.00
Pushing	1	True	False	250	RL Agent	65.7	0.93
Plugging	2	False	True	500	Motion Planner	147	0.98

TABLE I: **Task and Expert Summary.** # Obj: number of objects, Contact-rich: contact-richness between robot and objects, High-Fidel: High-fidelity task,  $T_L$ : time limit in simulation steps at 20 Hz, Expert Type: type of expert, Task Dur: average expert task duration in simulation steps, Exp SR: expert success rate during intervention.

expert, the task is initialized to a random initial configuration. If the robot neither queries nor completes the task after a time limit, automatic expert intervention takes place. After every  $N_d$  expert intervention has been made, we perform a policy update, which consists of policy training and threshold setting. The policy training involves training the policy from scratch, and threshold setting involves setting the base values from the training dataset for the OOD violation threshold used during robot-query decision-making. The full pseudo-code is available in Algorithm 1.

#### IV. EXPERIMENT

We address the following three research questions to understand the effectiveness of Diff-DAGger.

- RQ1** Can diffusion loss predict task failure (Section IV-B)?
- RQ2** Given a fixed number of expert interventions, can Diff-DAGger outperform existing methods (Section IV-C)?
- RQ3** Can Diff-DAGger reduce the wall-clock time of DAGger iterations (Section IV-D)?

##### A. Experiment Setup

1) *Tasks and Experts:* We include three tasks in simulation—stacking, pushing, and plugging—using the ManiSkill environment [19]. In the stacking task, the robot must pick up a red cube and place it on top of a green cube, testing its perception and basic manipulation ability. The pushing task requires the robot to push a red tee into a predefined position using an end-effector stick, presenting a challenge of contact-richness and explicit multi-modality in task completion. Finally, the plugging task requires picking up a charger and plugging it into a receptacle, posing a significant challenge of fine-manipulation with millimeter-level precision.

We design experts as either multi-modal or long-horizon planners to evaluate different expert types. Specifically, we use RL agents and motion planners as the experts: the motion planner, is a long-horizon planner that generates actions based on future goals, whereas multiple RL agents with different reward functions provide different modes for task completion. For stacking and plugging tasks, we use a rule-based RRT motion planner to simulate the expert [20]. For pushing, two experts are trained using PPO algorithm [21] with varying rewards: in addition to task-related reward, one agent is additionally rewarded for rotating the object clockwise direction, whereas other agent is rewarded for rotating counter-clockwise (2 Experts). We additionally compare learning from the counter-clockwise agent only (1 Expert). The tasks and experts are summarized in Table I.

2) *Baselines:* We compare Diff-DAGger to the following algorithms: Behavior Cloning, which uses the offline human demonstration data as the training data; Ensemble-DAGger, which uses five policies to calculate action variance for uncertainty estimation; and ThriftyDAGger [7], a SOTA robot-gated DAGger algorithm which incorporates risk measure into the decision rule using an offline RL algorithm. All methods use the diffusion policy with the same model architecture to ensure consistent expressiveness across methods.

3) *Model Details:* In all tasks, we use the CNN-based [22] diffusion policy with FiLM conditioning [23] for the observation. In our study, we test both state-based and image-based data: For the state-based case, we use the internal robot proprioception data (robot joint position and end-effector pose) and the ground-truth pose of the external objects as the input to the model. For the image-based case, we use a vision encoder to extract the embedding vector from the image and concatenate it with the proprioception data. Additionally, we use spatial-softmax instead of average pooling for the vision encoder [24]. All methods use position-based control, either with joint position control or end-effector pose control. For end-effector pose control, 6D representation for the orientation is used [25].

4) *Choices to Accelerate Learning:* Human-in-the-loop systems depend on the rapid training of robot policies, which necessitates fast policy learning. However, the original implementation of the diffusion policy is data-intensive, requiring hours of training [3]. In this section, we explore specific modifications that can significantly reduce the training time for diffusion policies.

First, the convergence rate of policy performance varies depending on the prediction type used for the diffusion model. We evaluate three prediction types—sample, epsilon, and V-objective—and find the V-objective [18] to be the best for training convergence. Secondly, using a small number of diffusion steps during training identical to the diffusion steps used for inference improves the convergence rate while not significantly affecting the policy performance. These choices enable the training to converge reasonably well in 300 epochs. Additionally, we set the observation horizon to one to reduce the amount of data processed in each batch. For image-based training, we use the lightweight R3M ResNet-

Task	$N_D$	Method	TP	TN	FP	FN	F1 ↑	Acc ↑
Stacking	20	Ours	29	59	10	2	<b>0.84</b>	<b>0.88</b>
		Ensemble-DAGger	27	33	37	6	0.55	0.60
		Thrifty-DAGger	33	30	34	3	0.49	0.63
Pushing (1 Expert)	50	Ours	29	51	9	11	<b>0.74</b>	<b>0.80</b>
		Ensemble-DAGger	38	10	52	0	0.59	0.48
		Thrifty-DAGger	37	6	57	0	0.57	0.43
Pushing (2 Experts)	25/25	Ours	27	51	8	14	<b>0.71</b>	<b>0.78</b>
		Ensemble-DAGger	15	45	5	35	0.43	0.60
		Thrifty-DAGger	25	38	15	22	0.57	0.63
Plugging	100	Ours	31	49	13	7	<b>0.76</b>	<b>0.80</b>
		Ensemble-DAGger	22	37	18	23	0.52	0.59
		Thrifty-DAGger	30	34	25	11	0.62	0.64

TABLE II: Confusion matrix comparing the binary robot query decisions (query or no query) with the binary task outcomes (success or failure) in 100 policy rollouts for visuomotor tasks. Here, *True Positive (TP)* is a query made to a failing episode. *True Negative (TN)* is a successful episode without query. *False Positive (FP)* is an unnecessary query made to a successful episode, and *False Negative (FN)* is a failure episode without query.  $N_D$  is the number of expert demonstrations used for training the policy. The numbers are chosen to ensure the policy can both succeed and fail during task execution.

18 model [26] and optionally freeze it to accelerate training at the cost of policy performance.

### B. Predictability of Robot Query on Task Failure

The effectiveness of a robot query system relies on how well it aligns with the actual need for expert intervention; Accurate predictions allow queries to be made only when necessary, avoiding both over-querying and under-querying. To quantitatively evaluate this, we use a confusion matrix between robot query decision and task outcome. For each task, we train the robot policy on a fixed number of expert demonstrations and rollout from 100 different initial configurations. We record task completion without expert intervention and whether the policy estimates high uncertainty during each episode, as described in Section III-C. All methods use the same set of thresholds, including  $\alpha$  and  $K$ , as shown in Table IV.

The results show that Diff-DAGger achieves a significant improvement over Ensemble-DAGger and Thrifty-DAGger in terms of its ability to predict task failure: Compared to Ensemble-DAGger, Diff-DAGger achieves 47% higher F1 and 45% greater accuracy scores on average across the visuomotor tasks. Compared to Thrifty-DAGger, Diff-DAGger improves F1 scores by 37% and accuracy by 43%. Notably, when learning from two pushing experts, both Ensemble-DAGger and Thrifty-DAGger yield high rates of false negative: This is because the action variance present in the training dataset is high due to diverging plans (clockwise paths and counter-clockwise paths) given the same state, resulting in the policies’ insensitivity toward true OOD data. In contrast, Diff-DAGger allow significantly lower rates of

	Stacking		Pushing (1 Expert)		Pushing (2 Experts)		Plugging	
	State	Image	State	Image	State	Image	State	Image
Behavior Cloning	0.83	0.85	0.92	0.87	0.91	0.91	0.73	0.68
Ensemble-DAGger	0.90	0.87	0.90	0.80	0.66	0.58	0.57	0.53
Thrifty-DAGger	0.88	0.87	0.85	0.78	0.77	0.73	0.69	0.60
Ours	<b>0.98</b>	<b>1.00</b>	<b>0.97</b>	<b>0.99</b>	<b>0.98</b>	<b>0.97</b>	<b>0.87</b>	<b>0.83</b>

TABLE III: Performance comparison across different tasks with state-based and image-based observations. We report the success rates using 100 environment configurations after the final iteration of DAGger. For each task, the number of expert demonstrations is fixed (detailed in Table IV) across methods. Our results show that Diff-DAGger consistently outperforms the other DAGger baseline methods given the same number of demonstrations from the expert.

Task	Action	$T_o$	$T_p$	$T_a$	$N_c$	RN18	PredTg	$T_d$	$N_i$	$N_f$	$N_d$	$\alpha$	$K$	$N_b$
Stacking	EEF	1	24	8	3	PT	V-obj	8	20	52	4	0.99	2	256
Pushing	Joint	1	24	2	1	FT	Epsilon	8	40	92	4	0.98	1	256
Plugging	EEF	1	48	16	3	FT	V-obj	64	20	100	8	0.99	3	256

TABLE IV: Hyperparameters for Diffusion Policy and DAGger. Action: action space,  $T_o$ : observation horizon,  $T_p$ : prediction horizon,  $T_a$ : rollout horizon,  $N_c$ : number of cameras, RN18: training strategy for vision encoder where PT means pre-trained and FT means fine-tuned, PredTg: prediction target when training diffusion policy,  $T_d$ : number of diffusion timesteps for training and inference,  $N_i$ : number of initial expert demonstrations,  $N_f$ : final number of expert demonstrations,  $N_d$ : number of expert intervention after each training session,  $K$ : patience for consecutive violation of threshold,  $N_b$ : Diff-DAGger specific batch size for calculating the expected diffusion loss.

false positive in other tasks, indicating its ability to handle multi-modality in demonstration data. The detailed results across tasks are shown in Table II.

### C. Task Performance

We evaluate the policy performance of methods for state-based and image-based observations. Diff-DAGger method consistently outperforms the baselines in task completion rate across tasks, assuming the same number of expert demonstrations is given. On average, Diff-DAGger achieves a 12.6% improvement over the second-best method in state-based tasks. For visuomotor tasks, Diff-DAGger on average achieves a 15.0% improvement over the other methods. Notably, Diff-DAGger achieves 100% policy performance with only 52 stacking demonstrations using image data, indicating that it can be used to significantly reduce the number of demonstrations required to train an optimal policy.

### D. Wall-Clock Time for DAGger

Diff-DAGger also significantly reduces wall-clock time for training, threshold setting and inference, in comparison to the Ensemble-DAGger-based methods. Whereas Ensemble-DAGger-based methods perform the ensemble action inference on the entire training data to set the numerical action variance threshold, Diff-DAGger requires passing a single batch per train data point to efficiently get the expected diffusion losses. Additionally, Diff-DAGger uses a single

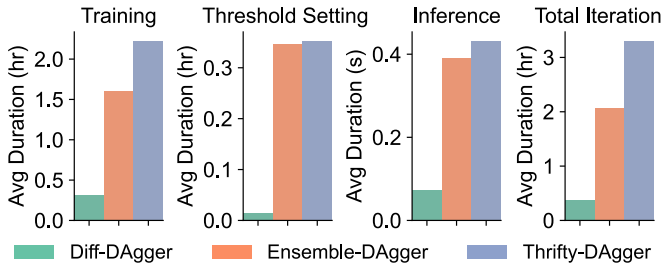


Fig. 4: Average duration for training, threshold setting, inference, and total iteration for different methods, when training a visuomotor policy for Stacking. A single A100 40 GB GPU is used. The initial and final number of demonstrations  $N_i$  and  $N_f$ , respectively, are 20 and 52, and training occurs after every  $N_d = 4$  interventions, with a total of 9 iterations.

policy, reducing the wall clock time for both training and inference by the factor of the number of policies used for ensemble. Thrifty-DAGger extends Ensemble-DAGger by estimating risk, requiring extra data collection using the robot policy and additional risk estimator training, resulting in longer wall-clock time across tasks.

We demonstrate these results on the visuomotor stacking task, where Diff-DAGger reduced training time by a factor of 5.1, threshold setting time by a factor of 24.5, and inference time by a factor of 5.3 compared to Ensemble-DAGger, as shown in Fig 2. The overall reduction in average policy update time is by a factor of 5.4, reducing the total time to just 0.37 hours. Thrifty-DAGger requires additional data collection and training for risk estimation, and Diff-DAGger achieves corresponding reduction factors for training, threshold setting, and inference times of 6.9, 24.9, and 8.8, respectively.

### E. Discussions

False positives and false negatives reported in Table II have distinct implications: a false positive means the robot unnecessarily asks for expert demonstration, simply losing the benefits of interactive learning and resembling offline imitation learning. In contrast, a false negative, where the robot overestimates its ability and fails, is more dangerous, as it can cause the robot to deviate significantly from desired states over time, diminishing the value of expert intervention data. Both Ensemble-DAGger and Thrifty-DAGger incur a high rate of false negative in most tasks and we speculate that this is the reason they perform worse than behavior cloning in many tasks. On the other hand, Diff-DAGger yields far fewer false negatives than other methods across tasks, making it a more suitable choice for an interactive learning framework. This increased sensitivity to task failure is visualized in Fig 5, where we show robot query behavior from each DAGger method. For instance, Diff-DAGger proactively requests expert intervention once the robots start to lose grip of the charger, while the other methods fail to detect this issue—resulting in either dropping the object or getting stuck in one motion.

We also observe an interesting emergent behavior from policies trained on Diff-DAGger collected data: recovery

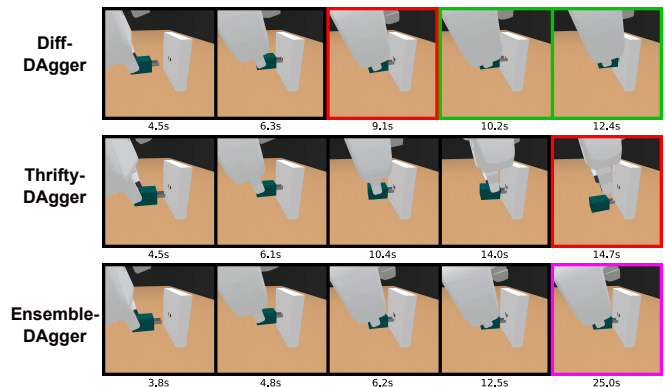


Fig. 5: Robot query modes for different methods in the plugging task. Black boxes indicate policy rollout, red boxes represent robot queries, green boxes are expert interventions, and the purple box marks an automatic expert intervention due to timeout. In Diff-DAGger (**Top**), the robot promptly queries the expert when the charger slips at 9.1s, leading to a successful episode with expert help. In Thrifty-DAGger (**Middle**), the robot continues to try plugging in despite slipping, eventually querying for intervention after dropping it at 14.7s. In Ensemble-DAGger (**Bottom**), the robot fails to query despite not progressing, and times out at 25.0s to trigger automatic expert intervention. Expert interventions for Thrifty-DAGger and Ensemble-DAGger are omitted due to space.

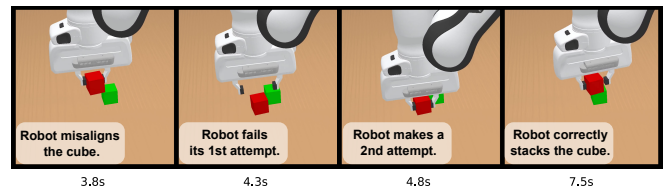


Fig. 6: Emergent behavior of DAGger-trained policy for stacking. We observed an interesting new behavior with Diff-DAGger trained policies: the recovery behavior after initial failure. This explains the improvement in policy performance over BC-trained policies.

behavior. As shown in Fig 6, after the policy fails at its initial attempt to stack the cube, it subsequently tries again and completes the task. This type of behavior is rarely seen when training the policy from offline behavior cloning, highlighting the effectiveness of Diff-DAGger.

### V. CONCLUSION & FUTURE WORK

In this work, we present Diff-DAGger, an efficient robot-gated DAGger method with diffusion policy. While Diff-DAGger shows improvements in task failure prediction, policy performance, and wall-clock time for learning over other methods, there are limitations: Whereas we dramatically reduce the wall-clock time for DAGger iteration, using an expressive policy class such as diffusion policy comes at the cost of increased training time in general. In addition, most of the choices we made to accelerate policy training is a trade-off between the policy performance, and we hope to address this in the future. Other future work includes learning from human experts for challenging real-world tasks. We hope that this work paves a way to open up more discussion for incorporating expressive policies into interactive learning frameworks in anticipation that computing will become faster over time.

## ACKNOWLEDGMENTS

This work was funded and supported by Delta Electronics Inc.

## REFERENCES

- [1] T. Z. Zhao, V. Kumar, S. Levine, and C. Finn, "Learning Fine-Grained Bimanual Manipulation with Low-Cost Hardware," in *Proceedings of Robotics: Science and Systems*, July 2023.
- [2] J. Ho, A. Jain, and P. Abbeel, "Denoising diffusion probabilistic models," *Advances in neural information processing systems*, vol. 33, pp. 6840–6851, 2020.
- [3] C. Chi, S. Feng, Y. Du, Z. Xu, E. Cousineau, B. Burchfiel, and S. Song, "Diffusion policy: Visuomotor policy learning via action diffusion," in *Proceedings of Robotics: Science and Systems*, July 2023.
- [4] S. Ross, G. Gordon, and D. Bagnell, "A reduction of imitation learning and structured prediction to no-regret online learning," in *Proceedings of the fourteenth international conference on artificial intelligence and statistics. JMLR Workshop and Conference Proceedings*, 2011, pp. 627–635.
- [5] R. Hoque, L. Y. Chen, S. Sharma, K. Dharmarajan, B. Thananjeyan, P. Abbeel, and K. Goldberg, "Fleet-dagger: Interactive robot fleet learning with scalable human supervision," in *Conference on Robot Learning*, 2023, pp. 368–380.
- [6] K. Menda, K. Driggs-Campbell, and M. J. Kochenderfer, "Ensembledagger: A bayesian approach to safe imitation learning," in *2019 IEEE/RSJ International Conference on Intelligent Robots and Systems (IROS)*. IEEE, 2019, pp. 5041–5048.
- [7] R. Hoque, A. Balakrishna, E. Novoseller, A. Wilcox, D. S. Brown, and K. Goldberg, "ThriftyDAGger: Budget-aware novelty and risk gating for interactive imitation learning," in *Conference on Robot Learning*, 2021.
- [8] S. Dass, K. Pertsch, H. Zhang, Y. Lee, J. J. Lim, and S. Nikolaidis, "Pato: Policy assisted teleoperation for scalable robot data collection," in *Proceedings of Robotics: Science and Systems*, 2023.
- [9] S. Ross and D. Bagnell, "Efficient reductions for imitation learning," in *Proceedings of the thirteenth international conference on artificial intelligence and statistics. JMLR Workshop and Conference Proceedings*, 2010, pp. 661–668.
- [10] M. Kelly, C. Sidrane, K. Driggs-Campbell, and M. J. Kochenderfer, "HG-DAGger: Interactive imitation learning with human experts," in *2019 International Conference on Robotics and Automation (ICRA)*. IEEE, 2019, pp. 8077–8083.
- [11] H. Liu, S. Dass, R. Martín-Martín, and Y. Zhu, "Model-based runtime monitoring with interactive imitation learning," in *International Conference on Robotics and Automation (ICRA)*, 2023.
- [12] J. Wong, A. Tung, A. Kurenkov, A. Mandlekar, L. Fei-Fei, S. Savarese, and R. Martín-Martín, "Error-aware imitation learning from teleoperation data for mobile manipulation," in *Conference on Robot Learning*, 2022, pp. 1367–1378.
- [13] S. E. Ada, E. Oztop, and E. Ugur, "Diffusion policies for out-of-distribution generalization in offline reinforcement learning," *IEEE Robotics and Automation Letters*, 2024.
- [14] J. Carvalho, A. T. Le, M. Baierl, D. Koert, and J. Peters, "Motion planning diffusion: Learning and planning of robot motions with diffusion models," in *IEEE/RSJ International Conference on Intelligent Robots and Systems (IROS)*. IEEE, 2023, pp. 1916–1923.
- [15] A. C. Li, M. Prabhudesai, S. Duggal, E. Brown, and D. Pathak, "Your diffusion model is secretly a zero-shot classifier," in *Proceedings of the IEEE/CVF International Conference on Computer Vision*, 2023, pp. 2206–2217.
- [16] S. Zhou, Y. Du, S. Zhang, M. Xu, Y. Shen, W. Xiao, D.-Y. Yeung, and C. Gan, "Adaptive online replanning with diffusion models," *Advances in Neural Information Processing Systems*, vol. 36, 2024.
- [17] B. Wang, G. Wu, T. Pang, Y. Zhang, and Y. Yin, "Diffail: Diffusion adversarial imitation learning," in *Proceedings of the AAAI Conference on Artificial Intelligence*, vol. 38, no. 14, 2024, pp. 15 447–15 455.
- [18] T. Salimans and J. Ho, "Progressive distillation for fast sampling of diffusion models," *arXiv preprint arXiv:2202.00512*, 2022.
- [19] T. Mu, Z. Ling, F. Xiang, D. Yang, X. Li, S. Tao, Z. Huang, Z. Jia, and H. Su, "Maniskill: Generalizable manipulation skill benchmark with large-scale demonstrations," *arXiv preprint arXiv:2107.14483*, 2021.
- [20] J. J. Kuffner and S. M. LaValle, "Rrt-connect: An efficient approach to single-query path planning," in *IEEE International Conference on Robotics and Automation*. IEEE, 2000, pp. 995–1001.
- [21] J. Schulman, F. Wolski, P. Dhariwal, A. Radford, and O. Klimov, "Proximal policy optimization algorithms," *arXiv preprint arXiv:1707.06347*, 2017.
- [22] O. Ronneberger, P. Fischer, and T. Brox, "U-net: Convolutional networks for biomedical image segmentation," in *Medical image computing and computer-assisted intervention—MICCAI 2015: 18th international conference, Munich, Germany, October 5-9, 2015, proceedings, part III 18*. Springer, 2015, pp. 234–241.
- [23] E. Perez, F. Strub, H. De Vries, V. Dumoulin, and A. Courville, "Film: Visual reasoning with a general conditioning layer," in *Proceedings of the AAAI conference on artificial intelligence*, 2018.
- [24] S. Levine, C. Finn, T. Darrell, and P. Abbeel, "End-to-end training of deep visuomotor policies," *Journal of Machine Learning Research*, vol. 17, no. 39, pp. 1–40, 2016.
- [25] Y. Zhou, C. Barnes, J. Lu, J. Yang, and H. Li, "On the continuity of rotation representations in neural networks," in *Proceedings of the IEEE/CVF conference on computer vision and pattern recognition*, 2019, pp.

5745–5753.

- [26] S. Nair, A. Rajeswaran, V. Kumar, C. Finn, and A. Gupta, “R3M: A universal visual representation for robot manipulation,” 2022.